FIGURE LEGENDS FOR SUPPLEMENTARY FIGURES

Figure S1. TCR Vβ usage of CD8$^+$ T cells in WT, K$^{b-/-}$D$^{b-/-}$ and K$^{b-/-}$D$^{b-/-}$M3$^{-/-}$ mice. Splenocytes isolated from WT, K$^{b-/-}$D$^{b-/-}$ and K$^{b-/-}$D$^{b-/-}$M3$^{-/-}$ mice were stained with antibodies against TCRβ, CD8, and indicated TCR Vβ chains. Bar graphs depict mean ± SEM for the percentage of TCRβ$^+$CD8$^+$ cells expressing particular TCR Vβ chains in WT (open bars), K$^{b-/-}$D$^{b-/-}$ (hatched bars) and K$^{b-/-}$D$^{b-/-}$M3$^{-/-}$ (filled bars) mice. Results shown are means from four mice per genotype. ∗, $p < 0.05$; ∗∗, $p < 0.01$; ∗∗∗, $p < 0.001$.

Figure S2. Kinetics of LM-specific CD8$^+$ T cell responses in K$^{b-/-}$D$^{b-/-}$M3$^{-/-}$ mice. Splenocytes were harvested from LM-infected K$^{b-/-}$D$^{b-/-}$ and K$^{b-/-}$D$^{b-/-}$M3$^{-/-}$ mice at various time points and stimulated *ex vivo* with HKLM for 7 h. Bar graph depicts mean ± SEM for the total number of IFN-γ-producing CD8$^+$ T cells from 9 mice per experimental group. ∗, $p < 0.05$; ∗∗∗, $p < 0.001$.

Figure S3. LM-specific CD8$^+$ T cells isolated from LM-infected K$^{b-/-}$D$^{b-/-}$M3$^{-/-}$ mice produce IFN-γ. Splenocytes and hepatic leukocytes were harvested from K$^{b-/-}$D$^{b-/-}$M3$^{-/-}$ mice 7 days post LM infection. Cells were stimulated with HKLM for 7 h and stained with antibodies against CD8β and TCRβ. Cells were then intracellularly stained for IFN-γ and analyzed by flow cytometry. Bar graphs depict the mean ± SEM for the percentage of CD8$^+$IFN-γ$^+$ cells within the TCRβ$^+$ gate. N=13 for untreated splenocytes as well as for HKLM-treated splenocytes.

Figure S4. LM-specific K$^{b-/-}$D$^{b-/-}$M3$^{-/-}$ CD8$^+$ T cells are not CD1d-restricted. Splenocytes were harvested from LM-infected K$^{b-/-}$D$^{b-/-}$ and K$^{b-/-}$D$^{b-/-}$M3$^{-/-}$ mice at 7 days post-infection and enriched for CD8$^+$ T cells. These T cells were then used as effectors in an IFN-γ ELISPOT assay. Uninfected or LM-infected BMDC were used as stimulators and were incubated with CD8$^+$ T cells in medium alone or in the presence of mAb against CD1d. Results are presented as the mean ± SEM of the number of

IFN-γ spot-forming units from two pooled animals per genotype and are representative of two independent experiments.

Figure S5. H2-M3-restricted CD8$^+$ T cell responses do not protect against secondary LM infection. $K^{b-/-}D^{b-/-}$ and $K^{b-/-}D^{b-/-}M3^{-/-}$ mice were infected with $2x10^3$ CFU of LM, then subsequently rechallenged with $5x10^4$ CFU of LM 1 mo following initial infection. Bacterial burden in the liver was determined at three days post secondary infection. Bar graphs depict the mean ± SEM for 7 mice per genotype.

Figure S6. LM-specific $K^{b-/-}D^{b-/-}M3^{-/-}$ CD8$^+$ T cells do not lyse Qa-1^b-expressing cells. Splenocytes were isolated from $K^{b-/-}D^{b-/-}M3^{-/-}$ mice 7 days post LM infection, enriched for CD8$^+$ T cells, and activated with ConA. After 3 days of ConA stimulation, splenocytes were used as effectors in a ^{51}Cr release CTL assay at an effector:target cell ratio of 30:1. Uninfected or LM-infected J774 cells, HeLa cells, or HeLa Qa-1^b-transfectants were labeled with ^{51}Cr and used as targets. Graph depicts the mean ± SEM for the percentage of LM-specific killing pooling two mice per genotype. Data are representative of two independent experiments.

Figure S1.

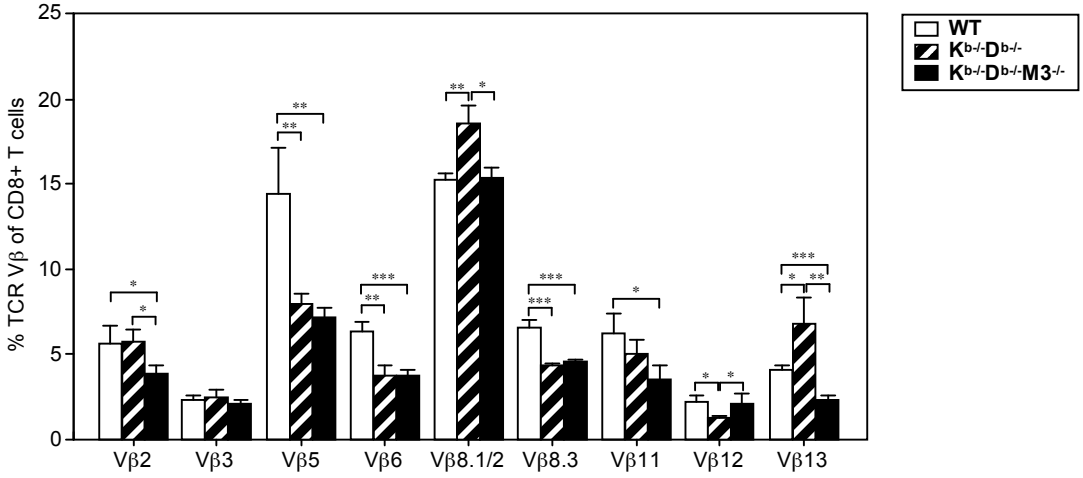

Figure S2.

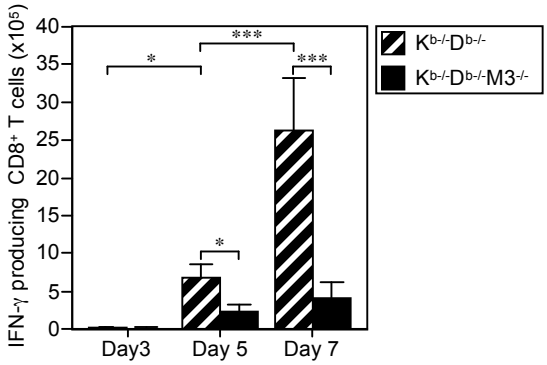

Figure S3.

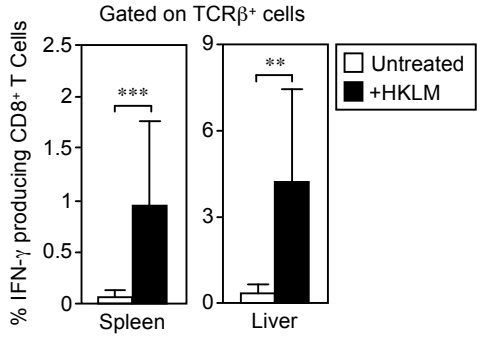

Figure S4.

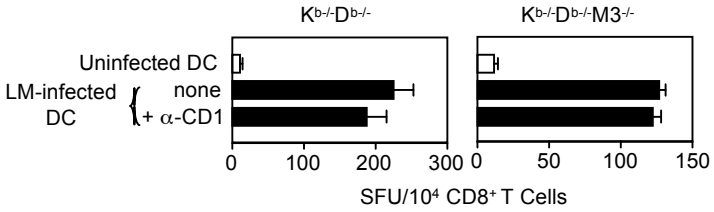

Figure S5.

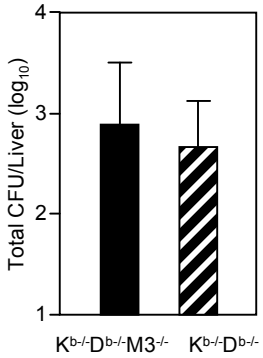

Figure S6.